Journal of Sol-Gel Science and Technology (2022) 101:37–45
https://doi.org/10.1007/s10971-021-05654-3

INVITED PAPER: SOL-GEL AND HYBRID MATERIALS WITH SURFACE MODIFICATION FOR APPLICATIONS

Texturing melting gels for water harvesting

S. Jenkins[1] · E. Sciarrone[2] · L. C. Klein[3]

Received: 19 March 2021 / Accepted: 23 September 2021 / Published online: 28 October 2021

Abstract

Organically modified silica gels that show melting gel behavior were coated on sand-blasted steel substrates. The gel surfaces were patterned using silicone rubber molds and nickel mesh. Grooved and hexagonally imprinted surfaces were compared to an unpatterned substrate for their ability to condense water from water vapor in humid air. The patterns of vertical lines were best able to condense the vapor in a way that lead to more liquid water collection per area. The motivation for studying patterned surfaces is to find ways to extend water harvesting capabilities in regions of low humidity.

Graphical Abstract

Sand-blasted steel substrate with melting gel coating, imprinted with vertical line pattern, showing water droplet formation when exposed to steam at an angle of 59°.

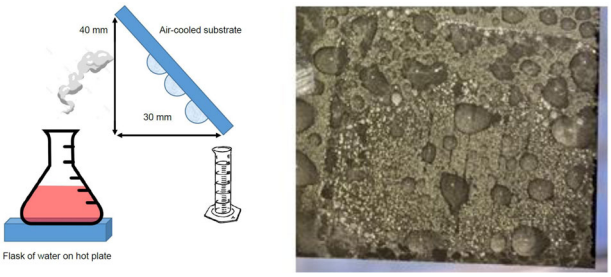

Keywords Melting gels · Melting gel coatings · Hydrophobic surfaces · Imprinted gels · Water harvesting

Highlights

- The surfaces of sand-blasted steel substrates have been patterned using melting gel coatings.
- Patterns of vertical lines in melting gels are capable of condensing water droplets from water vapor.
- Phenyl-modified melting gels can be patterned using silicone rubber molds with good fidelity.

1 Introduction

Lack of access to clean water is a leading cause of death, especially in dry areas, where rain and other sources of water are scarce. Only 3% of accessible water on earth is considered potable water. To increase supplies of clean water, one approach is the harvesting of atmospheric moisture. This can be done in small-scale projects instead of large-scale projects, which tend to have high costs associated with installation [1]. Atmospheric water harvesting is an alternative to filtration [2]. In this regard, melting gels

✉ L. C. Klein
licklein@soe.rutgers.edu

[1] Mechanical and Aerospace Engineering, Rutgers University, 607 Taylor Road, Piscataway, NJ 08854, USA

[2] Materials Science & Engineering, Clemson University, Clemson, SC 29634, USA

[3] Materials Science & Engineering, Rutgers University, 607 Taylor Road, Piscataway, NJ 08854, USA

have the distinct advantage among hybrid gel coatings that allows them to be patterned after the coating is in place. Also, melting gels, being hybrid gels, have surface energies that can be modified from hydrophobic to hydrophilic. Together the ability to pattern and the ability to adjust surface energy make melting gels candidate coatings for water harvesting.

Recently, there has been renewed interest in small scale projects for water harvesting. A reasonable goal for 1 square meter of collecting area is about 3.6 liters per hour. This collection rate is able to support one person. It is found that the efficiency of the water collection process is improved by using inclined patterned surfaces to facilitate water droplet formation [3, 4]. As the inclination increases, the droplets slide down faster, which increases the rate of water collection [5].

A crucial factor to consider when condensing water from the atmosphere is whether it condenses as a film or as droplets. In film-wise condensation, the surface over which water vapor condenses is hydrophilic. This film grows in thickness as it moves down the substrate, increasing the thermal resistance to heat transfer. This is shown schematically in Fig. 1. The latent heat is then transferred through the substrate, which reduces the rate that the water vapor condenses. The drops are not heavy enough to coalesce, so they stay in place until they eventually evaporate [5]. On the other hand, dropwise condensation usually occurs on hydrophobic surfaces when droplets with varying diameters condense on the substrate. As seen in Fig. 2, as the condensation continues, the droplets become larger and coalesce before rolling to the bottom of the surface, gathering the static beads along its downward trail [5]. During dropwise condensation, the bare surface is constantly exposed to the water vapor, as the action of the falling droplets, assisted by gravity, sweeps away the residual liquid. More drops nucleate on the surface, and this cycle continues [5]. Because the surface is exposed constantly to the water vapor, the heat transfer coefficient is higher for dropwise condensation [6]. Thus, dropwise condensation is preferred over film-wise condensation for water collection.

The state of a water droplet on a roughly textured surface affects its degree of hydrophobicity. The Cassie-Baxter state is attained when a liquid droplet remains on top of a textured pattern (Fig. 3), while the Wenzel state is attained when the liquid droplet spreads into the spaces within the pattern, as shown schematically in Fig. 4. While the Cassie-Baxter state is more common on hydrophobic surfaces than the Wenzel state, both states can occur on the same hydrophobic surface. A droplet may transition from Cassie-Baxter state to Wenzel state when droplet volume, surface vibrations, or surface inclination increases [7, 8].

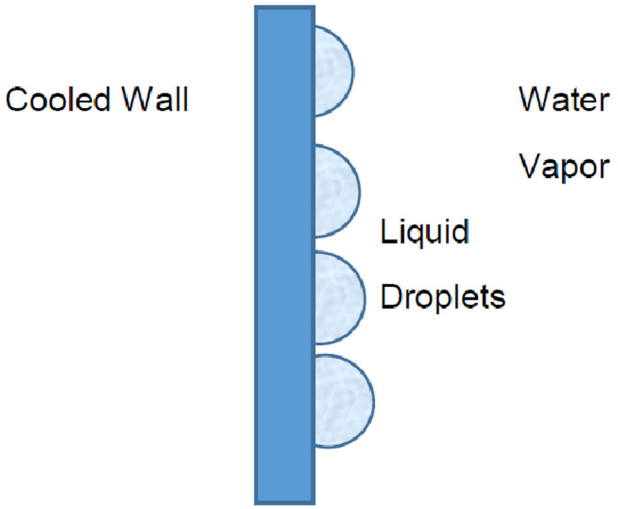

Fig. 2 Schematic of droplet formation when water condenses on a chilled surface and nucleates droplets

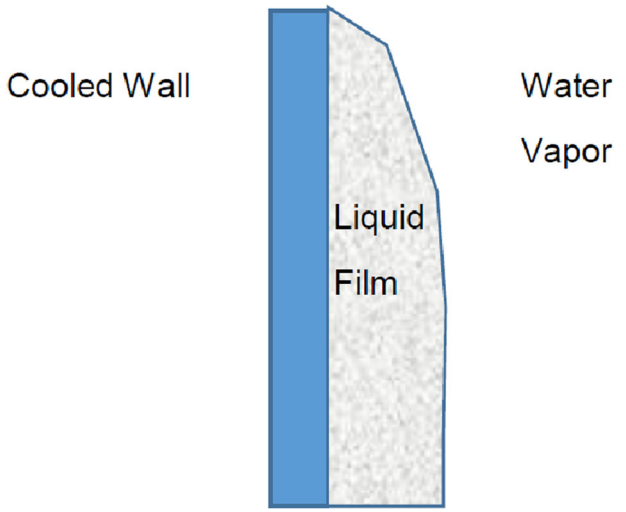

Fig. 1 Schematic of film formation when water condenses on a chilled surface

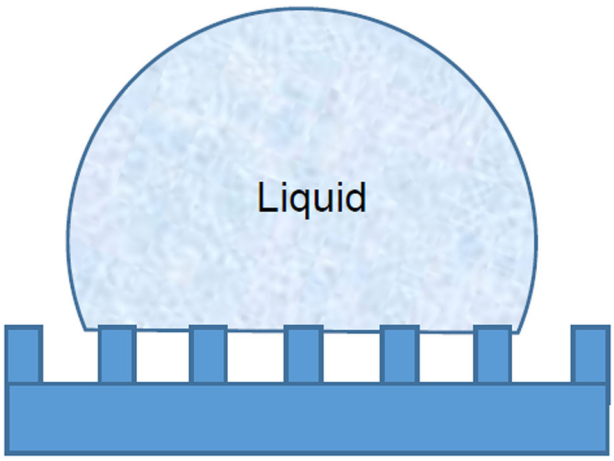

Fig. 3 Schematic of water drop on a textured surface showing Cassie-Baxter behavior

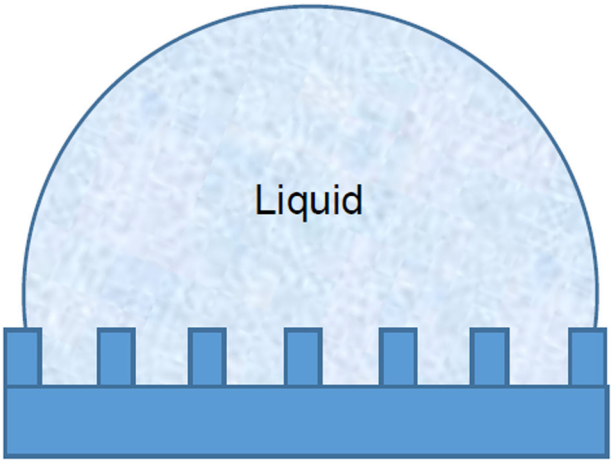

Fig. 4 Schematic of water drop on a textured surface showing Wenzel behavior

The contact angle θ of a water droplet on a substrate can be used to indicate hydrophilicity or hydrophobicity. A surface is considered hydrophilic if θ is <90°, while θ greater than 90° indicates a hydrophobic surface. The equation for contact angle is dependent on whether the droplet is in Cassie-Baxter state, where Eq. 1 is used:

$$\cos\theta = \mathrm{A}(\cos\theta + 1) - 1 \quad (1)$$

or the Wenzel state, in which Eq. 2 is used:

$$\cos\theta = 1 + [4A/(\alpha/\mathrm{H})]\cos\theta \quad (2)$$

where A is area, α is pillar width and H is pillar depth. For water harvesting, Cassie-Baxter behavior is desirable, such that a hydrophobic material is used to encourage droplet formation on a hydrophobic texture.

To adjust the surface energy of a gel coating, the surface composition can be modified with organic groups. Over the years, many methods have been used to incorporate silica into polymers or polymers into silica. The sol-gel process is one of the methods used to prepare composites of silica and polymers, especially when the majority component is silica [9]. The sol-gel process, requiring hydrolysis and polymerization of organically modified alkoxysilanes, leads to composites where the components are mixed on the nanoscale. Ordinarily, the outcome of the sol-gel process with a tetrafunctional precursor such as tetraethylorthosilicate ($Si(OC_2H_5)_4$ - TEOS) is a 3-dimensional network. With 4 identical groups attached to the Si, the sol-gel process eventually forms a gel, with structural elements reflecting pH and steric effects. However, 4 identical groups can be changed to, for example, 3 identical groups and one group with a direct Si-C bond. While the original groups are hydrolytically reactive, the substituted group, for example, methyl or phenyl, is hydrolytically stable.

The category of hybrid gels that is the main focus of this paper is melting gels [10]. They result from combinations of mono-substituted siloxanes and di-substituted siloxanes. For example, TEOS with one ethoxy substituted by a methyl can be combined with TEOS with two ethoxys substituted by methyls [11]. All mono-and di-substituted alkoxysilanes used in this study are listed in Table 1. The unsubstituted tetrafunctional alkoxysilane is included for comparison. The chemical formula, molecular weights and the % SiO_2 content of the precursors are listed.

Using a sol-gel process with a mono-substituted and a di-substituted alkoxysilane, where water is added in the parent alcohol, leads to a rigid, clear mass. Any excess water and alcohol are evaporated, but the gel does not shrink. When the gel is warmed to typically 110 °C (T_1), the gel softens to a clear liquid that easily flows and can be poured. When allowed to cool to room temperature, the gel returns to its rigid condition. The cycle of softening when warm and rigidifying when cool can be repeated many times. However, if the gel is heated to its crosslinking temperature ($T_2 > T_1$), it no longer softens, and the gel is no longer able to exhibit its so-called melting [12].

To show this behavior, what structures exist in the gel at the time the gel becomes rigid? By mixing different molar quantities of a precursor with 2 reactive groups with a precursor with 3 reactive groups, many structures can form. The simplest ones would be dimers, tetramers, silsesquioxanes, or ladders. The ladders would be the result of a reaction involving hydrolysis and condensation, leaving <50% of the original weight of the precursors. In fact, when unconsolidated gels are heated in a thermal analyzer, the measured weight loss is more in line with a nanocomposite, consisting of ladder structures with large amounts of retained organic groups [13]. Another study, where unconsolidated gels were dissolved in acetone, supports the idea that ladder-like chains form in gels before they crosslink to an irreversible solid [14].

If the melting gels are made up of chains that can move around when warmed to T_1, and only form additional crosslinks when heated to the consolidation temperature, T_{con}, then it is reasonable to expect melting gels to show the ability to soften and become rigid, and to repeat this cycle many times. Even after several years of storage in glass vials, samples continue to show this behavior. ^{29}Si NMR studies provide further support for ladder structures [15].

Differential scanning calorimetry (DSC) has been used to identify the glass transition temperature in melting gels, and these temperatures have been confirmed using oscillatory viscometry. All of the melting gels exhibit glass transition behavior in the way that polymer nanocomposites do, where domains of amorphous polymer exhibit relaxation phenomena. Glass transition temperatures as low as −50 °C were measured for the methyl triethoxysilane (MTES) -

Table 1 Phenyl-substituted precursors containing methoxy groups, listed in order of decreasing SiO_2 content, with TMOS and TEOS for comparison

Precursor	Chemical formula	Molecular weight	%SiO_2	Number of reactive groups
Tetramethoxysilane TMOS	$C_4H_{12}O_4Si$	152.22	39.5	4
Tetraethoxysilane TEOS	$C_8H_{20}O_4Si$	208.33	28.8	4
Phenyltrimethoxysilane PhTMS	$C_9H_{14}O_3Si$	198.29	30.3	3
Diphenydimethoxysilane DPhDMS	$C_{14}H_{16}O_2Si$	244.36	24.6	2

dimethoxydiethoxysilane (DMDES) system [11]. The glass transition is generally thought of as the interval of transition between liquid and glassy states. As such, the T_g should increase with an increase in the number of oxygen bridges between silicon atoms [16].

Turning now to the application of melting gels in water harvesting, there has been considerable interest in finding textured surfaces that are able to attract atmospheric water and facilitate the nucleation of water droplets. Many materials have been investigated including metals, polymers and composites. The key aspect of the surfaces is the ability to pattern on the microscale and macroscale [17]. Even the nanoscale has been investigated to improve efficiency [18, 19]. The parameters that alter the hydrophilicity or hydrophobicity have been adjusted by changing the surface chemistry and the scale of the pattern [20, 21]. These studies indicate that it is desirable to find methods for patterning surfaces that can be scaled up. Imprinting with melting gels falls in the category of being scalable.

The use of imprint lithography on melting gels has been demonstrated in the past. While melting gels were developed originally to replace low melting inorganic glasses, new applications and functionalities have appeared [22–24]. The refractive index of hybrid coatings was found to vary according to the quantity of the organic bonded to the inorganic network, making them candidates for waveguides. One of the earliest examples of imprinting melting gels involved a waveguide that was prepared by microfluidic lithography, based on phenyltriethoxysilane (PhTES), MTES and TEOS [22]. Using this method, patterned microstructures were obtained with a linewidth of 20 and 35 µm. In another study, pregrooves 1.6 µm in pitch and 86 nm in depth were patterned on a 130 mm diameter glass disk substrate for optical data storage using MTES and TEOS [23]. Other properties of melting gels that have been reported are their surface chemistry as indicated by water contact angle measurements, gas transmission properties in hermetic seals, and dielectric properties [25].

When it comes to preparing textured surfaces, other techniques have been used such as step-and-flash imprint lithography (SFIL), e-beam lithography, and post-forming surface treatment [17, 26]. More complicated patterns have been imitated from various plants and organisms [27–29].

The value of using imprint lithography in melting gels is seen in the relationship:

$$z = \left(\frac{R\,\sigma\,t\cos\theta}{2\eta}\right)^{1/2} \tag{3}$$

where z is the maximum feature height/wall height, R is the periodic groove radius/width of channel, θ is the contact angle with the PDMS mold (<90°), and σ is the viscosity during forming. For interface energy between the PDMS and gel, the surface energy σ is estimated to be about 0.02 N m^{-1} [30]. For the combination of melting gel and PDMS mold, the features conveniently fall between 0.1 mm and 1.0 mm, which are suitable for water harvesting operations.

The composition selected for this imprint study contains 80 mol% PhTMS-20 mol% DPhDMS with small additions of TEOS to control thickness, based on a previous study [31]. Samples were prepared by pouring the softened gel into a 2.54 cm neoprene rubber o-ring that was stuck with a superglue to PET film. The gel was warmed to about 75 °C by immersing a glass vial of gel in warm water. When the viscosity of the gel was as low as that of water, the gel was poured. Two or three samples were poured before the gel became too thick to pour. The gel filling the o-ring was slightly concave upward, indicating a high contact angle between the gel and the rubber o-ring. After the sample was heated at 175 °C for 5 min, it was hard and glassy.

When it was re-softened, a pattern was imprinted on the surface manually. A simple pattern of parallel lines was pressed into the sample for a few seconds to make the imprint, and then removed. If the sample was warmed slightly, the imprint healed and disappeared. If the sample was cooled to room temperature, the imprint remained, with good fidelity. The samples were scanned with a profilometer, and the periodicity of the pattern was preserved. The features were on the 100 micron scale [31].

There has been considerable progress in the past 10 years to develop the concept of imprint lithography, as well as UV lithography, with melting gels and hybrid gels [32]. In addition, melting gels are suitable for embossing and capillary molding [33, 34]. In one such test, a polydimethyl siloxane (PDMS) stamp pattern was transferred to a 80 mol% PhTES-20 mol% DPhDES gel. A typical result of the capillary molding process is a pattern of the mold is

replicated and the walls maintain a high aspect ratio of 5:1 [35]. Other patterning techniques required a slurry or used the gel itself as the rubber stamp [36, 37]. In the present study, a survey of techniques was carried out, along with a sampling of melting gel formulations that have been described in the past. Some trends were found quickly with regard to compositions that were suitable. Only the results from these trials are reported. Also, while several textures were examined, only the results from grooved samples are included [38].

2 Experimental

2.1 Preparing melting gels

For methyl substituted melting gels, the preparation steps have been reported in detail [11]. These compositions were not investigated further as surfaces for water harvesting because they were too hydrophobic. On the other hand, the phenyl-substituted melting gels were in the right range of surface energies. For the phenyl substituted systems, a two-step synthesis was used [12]. First the mono-substituted alkoxysilane and water were mixed together. The molar ratio of PhTMS:H_2O was 1:1.5. The pH of the water was adjusted to 2.5 using a 0.1 N HCl solution. After the water was added to the PhTMS, the mixture was stirred at 40 °C in a covered beaker. In the absence of a co-solvent, the mixture initially showed immiscibility between water and PhTMS. However, a clear solution was obtained after 30 min of stirring.

In the second step, the di-substituted alkoxysilane DPhDMS was diluted with methanol. The molar ratio of DPhDMS:CH_3OH was 1:4. The DPhDMS-methanol mixture was added dropwise to the clear solution of PhTMS and water. This mixture was stirred for another two hours in a closed beaker at 40 °C. Then, the clear solution was cooled to room temperature and stirred overnight in an open system until gelation occurred. The gels were then dried at 70 °C for 24 h, followed by a heat treatment at 110 °C. After these heat treatments and cooling, the gels were rigid at room temperature, but they re-softened at ~110 °C. The consolidation temperature for the composition 80 mol% PhTMS-20 mol% DPhDMS was 170 °C, and this composition was studied for its moldabillity.

The compositions used in this study were modified with small TEOS additions [38]. The base composition listed above had 2 and 10 mol% addition of TEOS, based on one mole of PhTMS. The sample with 2 mol% was poured onto the substrate when it was fluid. The sample with 10 mol% was broken into a powder, and the powder was allowed to viscous sinter onto the substrate by heating to the softening temperature. For the sample with 2 mol% TEOS, the T_g was 13 °C and its T_{con} (consolidation temperature) was 215 °C. For the sample with 10 mol%, the T_g was 24.5 C and its T_{con} was 195 °C. Their densities were about the same at 1.29 g/cm^3, and the sample with 10 mol% took 13 h to gel, compared to 12 h for 2 mol%. The static contact angle with water was 91° for 2 mol% and 88° for 10 mol%. Sliding angles were not measured, but their measurement in future studies is critical to understanding the ability to harvest water.

2.2 Patterning melting gels

To create a texture or pattern on the gel, a variety of molds were tried to find which molds could withstand heating at 190 °C for 24 h and be removed from the gel without the gel adhering to it. Two commercial silicone rubbers (Moldstar30™ and Ecoflex™) were tried, with the stiffer rubber (Moldstar30™) being better (Smooth-On, Inc., Macungie, PA 18062). The mold with vertical lines is shown in Fig. 5. In addition, a 2.54 cm circular nickel screen with a honeycomb grid pattern was used.

To prepare the sample, the gel was heated in a glass vial to 110 °C in a beaker of water on a hot plate. When the gel became fluid, the vial was removed and the gel was poured directly onto the sandblasted steel substrate. The nickel screen and the Moldstar30™ silicone mold with a simple line pattern were pressed into the gel. Part of the sample was left unpatterned. Then the substrate was placed into an unheated oven and heated to 190 °C. The gels were held for 24 h and left to cool to room temperature for 8 h before being taken out of the oven. The molds were then carefully removed.

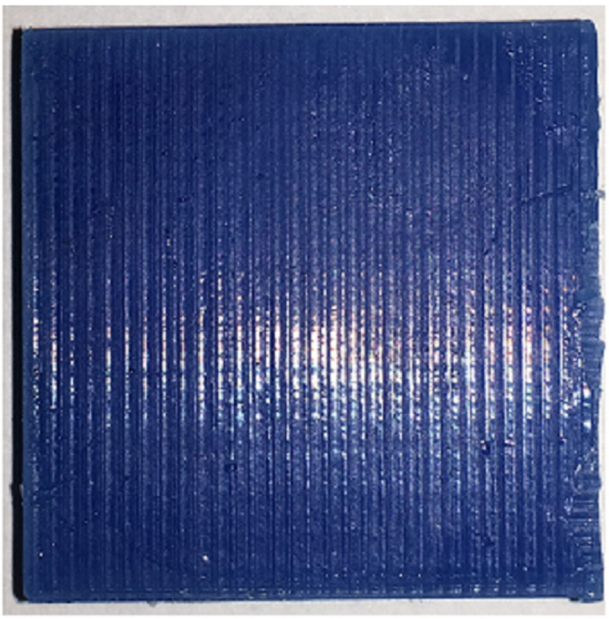

Fig. 5 Moldstar30™ silicone rubber with pattern of vertical lines (about 2.5 cm x 2.5 cm)

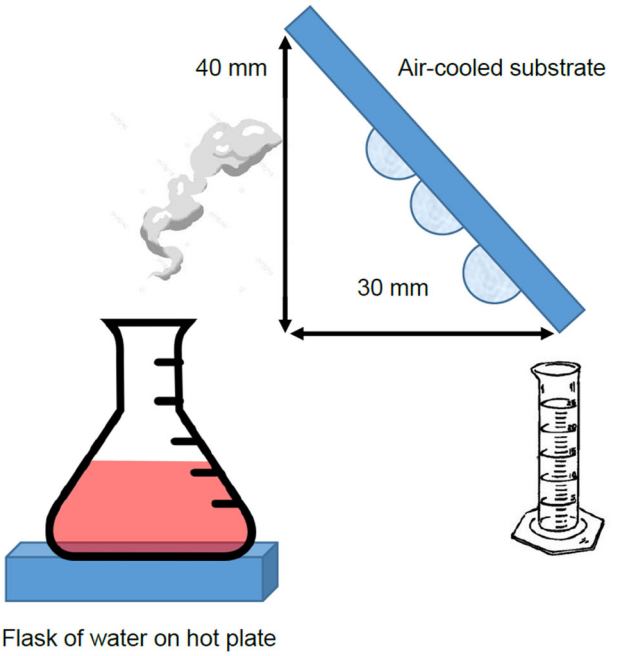

Fig. 6 Set-up of apparatus for condensing water vapor and collecting run off, with sample tilted at approximately 59°

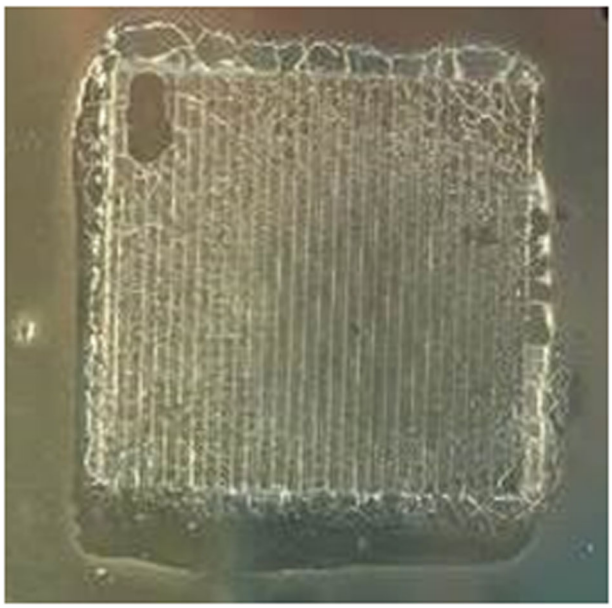

Fig. 7 Imprint in melting gel from Moldstar30™ pattern

2.3 Collecting water from patterned surfaces

To test the water-condensing abilities of the surfaces, a flask filled with water and a few drops of food coloring was boiled on a hot plate. The Erlenmeyer flask was capped with a rubber stopper threaded with a flexible tube, which was directed towards the underside of the substrate. Copying the set up used in other studies, the underside of the substrate was used for condensation [8]. When the water reached a boil, the steam in the tube was directed at each of the various patterns. The topside of the substrate was positioned in front of an air conditioner to facilitate cooling. The experimental set up is shown in Fig. 6.

The use of boiling water as a vapor source and an air conditioner for active cooling produced measurable quantities of water collected over a 2 h period. These conditions allowed for the determination of preferred patterns in a qualitative and a quantitative way. Images of the collecting surface could be obtained easily with a camera, and the presence or absence of droplets was observed. Further analysis of the images could be carried out to determine average droplet size and size distribution, but that has yet to be performed.

The substrate was tilted initially at a 75° angle on top of a graduated cylinder that was used to collect the run off. The condensation was observed and photographed every five minutes. The amount of water collected in the graduated cylinder was measured every 30 min. These measurements were recorded for 2 h. The patterns were used concurrently as well as separately. By adjusting the angle of tilt, it was found empirically that the best results were obtained when the angle was decreased to 59°. This angle was used for the subsequent samples and each run was repeated twice.

3 Results

The imprint on the gel with composition 80 mol% PhTMS-20 mol% DPhDMS and 2 mol% TEOS after heating at 190 °C is shown for the vertical lines in Moldstar30™ (Fig. 7), along with the honeycomb pattern created with a nickel mesh screen (Fig. 8). The lines in the Moldstar30™ material are about 1 mm apart. The patterned gel was scanned in a profilometer to confirm that the lines were separated by about 1 mm and had a depth of about 0.1 mm. This is consistent with the features on the Moldstar30™ stamp. Because the honeycomb pattern tended to show film wise condensation, no data are reported from the time studies. All of the patterns are shown on sand-blasted steel substrates.

Through qualitative analysis of the camera images, it was determined that the simple line patterned gel surface experienced dropwise condensation, forming large droplets. The droplets on the line pattern had the largest average size per time interval and the highest contact angle, which in fact produced the most water (Fig. 9). The honeycomb pattern (Fig. 10) formed small water droplets, but also created a film in the middle of the pattern. The collection rates from this pattern were erratic.

Better results were obtained when each sample was studied individually. Measurements collected over 2 h at 30 min intervals showed approximately linear behavior. These results are plotted in Fig. 11. In side-by-side trials, the rates of water collection were calculated from the slopes

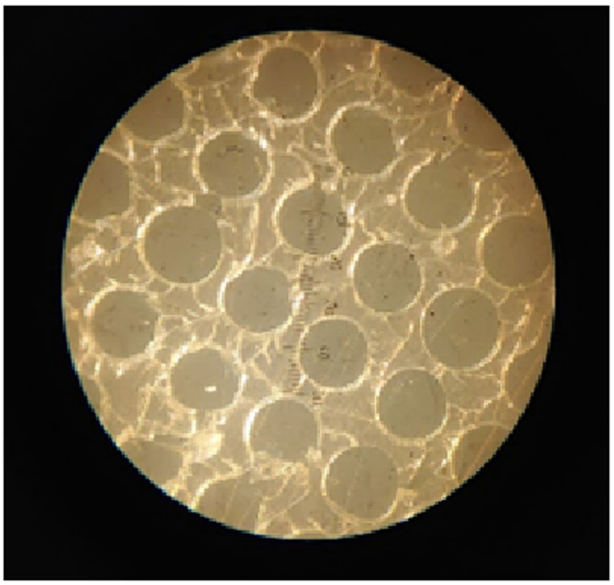

Fig. 8 Imprint in melting gel from nickel mesh

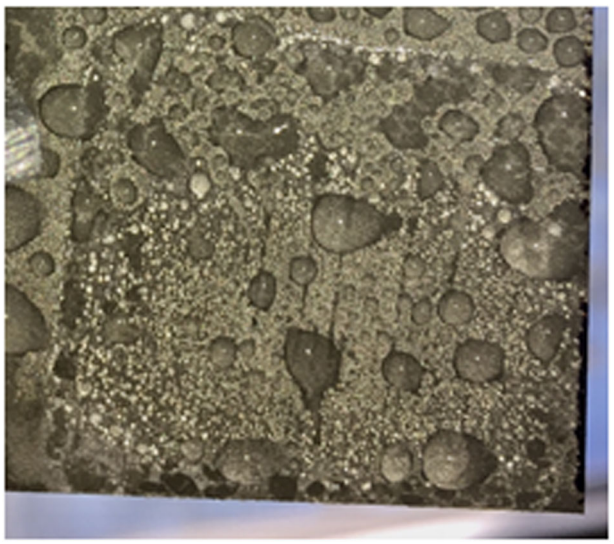

Fig. 9 Water droplets forming on line pattern

of the water volume vs. time plots for 1 h of collection. Each sample was repeated, and an unpatterned surface was used for comparison. These values are collected in Table 2. The samples were not dried or cleaned between the trials, which may account for the larger discrepancies between trials on the honeycomb and unpatterned surfaces. These surfaces formed films, where the vertical lined surface formed droplets.

It was observed that when the surface inclination was increased, the liquid droplets transitioned from Cassie-Baxter state to Wenzel state. Therefore, the inclination was maintained at 59° for the remaining trials. On a consistent basis, it was found that the line pattern resulted in the most water collected and with an average rate almost 2 times higher than the other

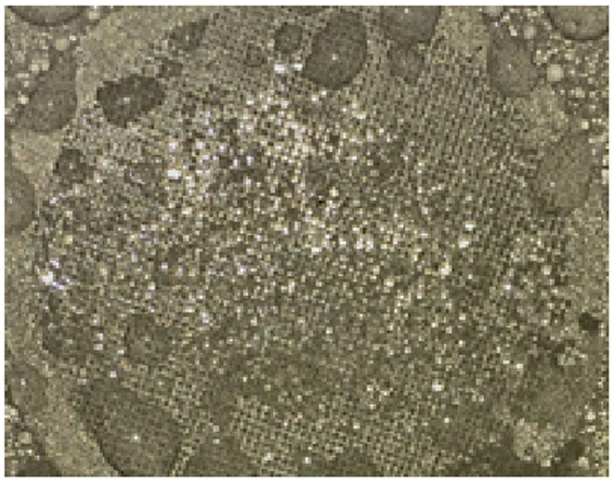

Fig. 10 Droplets and film formation on honeycomb pattern

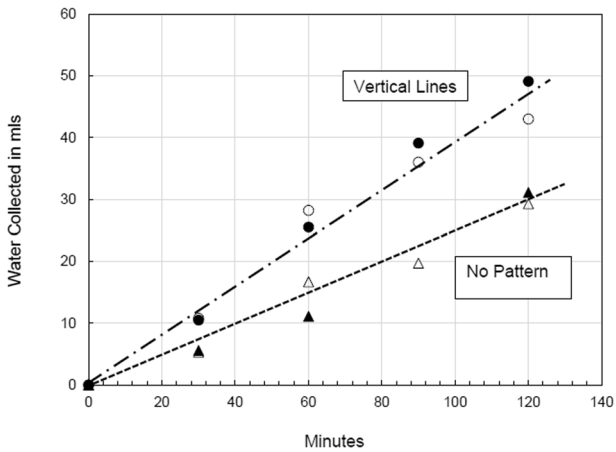

Fig. 11 Comparison of water collection results from samples with coatings (triangles) and without coatings (circles), first (open) and second (filled) trials

surfaces. In all cases listed in Table 2, the R^2 values were close to 1, indicating little scatter from best fit straight lines.

In addition, it was noted that the water that collected from all of the substrates was clear. Since the boiling water contained food coloring, it was encouraging to see that the collected water did not have residual color.

4 Discussion

While it was expected that the textured surfaces would increase the collection of water, based on the considerations of contact angle, and the criteria for Wenzel or Cassie-Baxter behavior, the magnitude of the effect was not known until it was measured. The surface with the vertical lines gave more consistent behavior when the measurements were repeated. There was no reduction in the quantity of water collected from the first trial to the second trial. Further

Table 2 Summary of water collection rates for repeat trials with patterned melting gel surfaces, with unpatterned surface for comparison

	Vertical lines ml/hr	R^2	Honeycomb ml/hr	R^2	Unpatterned ml/hr	R^2
Trial 1	10.4	0.991	11.3	0.992	8.40	0.995
Trial 2	11.0	0.993	7.62	0.992	5.58	0.959

trials are needed to establish long term performance. Another comparison of the surface with vertical lines showed almost twice the rate for the surface with lines compared to the surface with gel but no lines. Other patterns such as those described as pillars, mushrooms, pyramids and truncated pyramids may be even better with regard to Cassie-Baxter behavior, but these patterns are more complicated to imprint on the surface [39].

Since the melting gels have surface energies that place them at the boundary between hydrophilic and hydrophobic, the role of texture is significant. Generally, increased roughness on hydrophilic surfaces leads to a decrease in the contact angle, while increased roughness on hydrophobic surfaces leads to a decrease in the contact angle. The collection of water droplets from these surfaces is sensitive to this interaction. The patterns with the lines gave the best compromise of surface energy and roughness, leading to primarily Cassie-Baxter behavior.

In addition to the sensitivity to roughness, there is a relationship between the ability to nucleate water droplets and the ability to dissipate the heat of vaporization. The models for thermal heat balance are far more complicated than the qualitative observations made in this study. Nevertheless, the ability to dissipate the heat using the metal substrate and the active cooling permitted the evaluation of the surface patterns. The coatings themselves were relatively thin, <1 mm, and did not interfere with heat transfer. A more in-depth model of the heat flow in this system would be beneficial. In addition, studies in much lower relative humidities (<40%) are essential to show the performance in conditions more likely to exist in arid climates.

The rates of collection are about 10 ml per hour for an area of about 1 cm^2. If the recommended collection is 3.6 liters per hour for 1 m^2, then this scales to 10^6 ml or 1000 l. Of course, the set up directs saturated steam at a cooled substrate in near proximity. The ease of droplet formation is readily seen on the patterned surface. Further work is needed to understand the nucleation efficiency of water droplets on the vertical lines pattern.

5 Conclusions

Using the principles of the Cassie-Baxter and Wenzel behavior of water on a patterned surface, it was found that the vertical line pattern was more effective than either the honeycomb pattern or the sand blasted surface in collecting water. Condensation occurred on all of the surfaces, but the collection and rolling of droplets was easier on the surface with the lines. The honeycomb surface, compared to the sand-blasted surface and the surface with vertical lines, produced smaller droplets and had a tendency for film formation. Larger droplets are needed to take advantage of the effects of gravity, so that the water rolls down the inclined substrate and coalesces with other droplets, after which they collectively proceed down the substrate. This leaves behind uncovered surface on the substrate for more drops to nucleate.

Other factors, such as the convex shape of the line pattern and relative areas of the two patterns, may contribute to the amount of water collected. It is also noteworthy that the collected water did not have evidence of the food coloring that was in the source water. Through the process of boiling, evaporating, and condensing the water, contaminants were removed by distillation from the water.

Given the critical need for pure drinking water, further research on the topic of water harvesting is required. Continued research would allow for experimentation in humid conditions and a controlled environment. The implementation of the experiment in more realistic settings would ensure a more accurate analysis of its applicability. According to the results of this experiment, there is a linear relationship between the amount of water collected and time elapsed for a given area of exposure. Thus, the experiment has the potential for scale up. The idea is that with a properly patterned surface and a large enough area of exposure, this method of water harvesting can be deployed in many places. A distinct advantage is that it contains no moving parts.

Acknowledgements Financial support was received from the Rutgers Aresty Honors Program (SJ) and NSF-REU DMR-1659099 (ES). The authors acknowledge the contributions of the participants of the 2019 NJ Governor's School in Engineering and Technology, Emily Tsai, Lara Vaz, and Alan Yeung.

Compliance with ethical standards

Conflict of interest The authors declare no competing interests.

References

1. Cain NL (2014) A different path: the global water crisis and rainwater harvesting. Consilience: J Sustain Dev 12:147–157

2. Wessel L (2019) How humans get in the way of clean water. Scientific American 282 (Jan)
3. Zheng S, Eimann F, Philipp C, Fieback T, Gross U (2020) Experimental and modeling investigations of dropwise condensation out of convective humid air flow. Int J Heat Mass Transf 151:119349 16p
4. Sikarwar BS, Battoo NK, Khandekar S, Muralidhar K (2011) Dropwise condensation underneath chemically textured surfaces: simulation and experiments. J Heat Transf 133:021501 15p
5. Wilkins DG, Bromley LA, Read SM (1972) Dropwise and film-wise condensation. AIChE J 19:119–123
6. El Fil B, Kini G, Garimella S (2020) A review of dropwise condensation: theory, modeling, experiments and applications. Int J Heat Mass Transf 160:120172 21p
7. Xie J, Xu J, Shang W, Zhang KI (2018) Dropwise condensation on superhydrophobic nanostructure surface part II: Mathematical model. Int J Heat Mass Transf 127:1170–1187
8. Shirsath GB, Muralidhar J, Pala RGS, Ramkumar J (2019) Condensation of water vapor underneath an inclined hydrophobic textured surface machined by laser and electric discharge. Appl Surf Sci 484:999–1009
9. Avnir D, Klein LC, Levy D, Schubert U, Wojcik AB (1998) Organo-silica Sol-Gel Materials. In: Rappoport Z, Apeloig Y (eds.) The Chemistry of Organosilicon Compounds Vol. 2. Wiley, London, p 2317–2362
10. Klein LC, Jitianu A (2011) Organic-inorganic hybrid melting gels. J Sol-Gel Sci Tech 59:424–431
11. Jitianu A, Doyle J, Amatucci G, Klein LC (2010) Methyl modified siloxane melting gels for hydrophobic films. J Sol-Gel Sci Tech 53:272–279
12. Jitianu A, Amatucci G, Klein LC (2009) Phenyl-substituted siloxane hybrid gels that soften below 140 °C. J Am Ceram Soc 92:36–40
13. Jitianu J, Lammers K, Arbuckle-Keil GA, Klein LC (2012) Thermal analysis of organically modified siloxane melting gels. J Therm Anal Calorim 107:1039–1045
14. Ashraf KM, Matsumoto S, Kurumada K (2012) Determination of heat treatment temperature for completing polycondensation of vinyl substituted silica particles prepared by sol-gel method. Chem Eng Technol 35:2155–2160
15. Jitianu A, Cadars S, Zhang F, Rodriguez G, Picard Q, Aparicio M, Mosa J, Klein LC (2017) ^{29}Si NMR and SAXS investigation of the hybrid organic-inorganic glasses obtained by consolidation of the melting gels. Dalton Trans 46:3729–3741
16. Klein LC, Al-Marzoki K, Jitianu A (2017) Phase separation in melting gels. Phys Chem Glasses: Eur J Glass Sci Technol B 58:142–149
17. Abolghasemibizaki M, Robertson CJ, Fergusson CP, McMasters RL, Mohammadi R (2018) Rolling viscous drops on a non-wettable surface containing both micro- and macro-scale roughness. Phys Fluids 30:023105 7 p
18. Zhao F, Zhou X, Shi Y, Qian X, Alexander M, Zhao X, Mendez S, Yang E, Qu L, Yu G (2018) Highly efficient solar vapour generation via hierarchically nanostructured gels. Nat Nanotechnol 13:489–495
19. Wang Z, Owais A, Neto C, Pereira JM, Gan Y (2020) Enhancing spontaneous droplet motion on structured surfaces with tailored wedge design. Adv Mater Interfaces 2000520 8p
20. Lee J, So J, Bae WG, Won Y (2020) The design of hydrophilic nanochannel-macrostripe fog collector: enabling wicking-assisted vertical liquid delivery for the enhancement in fog collection efficiency. Adv Mater Interfaces 7:1902150 9p
21. Zhao Y, Preston DJ, Lu Z, Queeney J, Wang EN (2018) Effects of millimetric geometric features on dropwise condensation under different vapor conditions. Int J Heat Mass Transf 119:931–938
22. Jeong S, Ahn SJ, Moon J (2005) Fabrication of patterned inorganic-organic hybrid film for the optical waveguide by microfluidic lithography. J Am Ceram Soc 88:1003–1036
23. Matsuda A, Matsuno Y, Tatsumisago M, Minami T (1998) Fine patterning and characterization of gel films derived from methyltriethoxysilane and tetraethoxysilane. J Am Ceram Soc 81:2849–2852
24. Masai H, Takahashi M, Tokuda Y, Yoko T (2005) Gel-melting method for preparation of organically modified siloxane low-melting glasses. J Mater Res 20:1234–1241
25. Gambino L, Jitianu A, Klein LC (2011) Dielectric properties of organically modified siloxane melting gels. J Non-crystalline Solids 358:3501–3504
26. Mele E, Di Benedetto F, Persano L, Pisignano D, Cingolani R (2005) Combined capillary force and step and flash lithography. Nanotechnology 16:391–395
27. Ang BTW, Zhang J, Lin GJ, Wang H, Lee WSV, Xue J (2019) Enhancing water harvesting through cascading effect. ACS Appl Mater Interfaces 11:27464–27469
28. Xu S, Wang Q, Wang N (2021) Chemical fabrication strategies for achieving bioinspired superhydrophobic surfaces with micro and nanostructures. Adv Eng Mater 23:2001083 (21 p)
29. Wang J, Yi S, Yang Z, Chen Y, Jiang L, Wong CP (2020) Laser dorect structuring of bioinspired spine with backward microbarbs and hierarchical microchannels for ultrafast water transport and efficient fog harvesting. ACS Appl Mater Interfaces 12:21080–21087
30. Mondal S, Phukan M, Ghatak A (2015) Estimation of solid-liquid interfacial tension using curved surface of a soft solid. PNAS 112:12563–12568
31. Klein LC, McClarren B, Jitianu A, Silica-Containing Hybrid Nanocomposite "Melting Gels" In: Thermec 2013 Symposium on Advanced Protective Coatings/Surface Engineering, ed. B. Mishra, M. Ionescu. And T. Chandra, Materials Science Forum, Trans Tech Publishers, Vol. 783–786, 2014, pp. 1432-1437
32. Back F, Bockmeyer M, Rudigier-Voigt E, Lobmann P (2013) Hybrid polymer sol-gel material for UV-nanoimprint: microstructure and thermal densification. J Sol-Gel Sci Technol 66:73–83
33. Kim E, Xia Y, Whitesides GM (1996) Micromolding in capillaries: applications in materials science. J Am Chem Soc 118:5722–5731
34. Letailleur A, Teisseire J, Chemin N, Barthel E, Søndergard E (2010) Chemorheology of sol-gel silica for the patterning of high aspect ratio structures by nanoimprint. Chem Mater 22:3143–3151
35. Fernandez-Sanchez C, Cadarso VJ, Darder M, Dominguez C, Llobera A (2008) Patterning high-aspect-ratio sol-gel structures by microtransfer molding. Chem Mater 20:2662–2668
36. Ikeda H, Fujino S, Kajiwara T (2011) Fabrication of micropatterns on silica glass by a room-temperature imprinting method. J Am Ceram Soc 94:2319–2322
37. Schmidt M, Philippi M, Munzer M, Stangl JM, Wieczorek R, Harneit W, Muller-Buschbaum K, Enke D, Steinhart M (2018) Capillary nanostamping with spongy mesoporous silica stamps. Adv Funct Mater 28:1800700 9p
38. Al-Marzoki K, Klein LC, Jitianu A (2020) Effect of tetra-ethoxyethoxysilane on melting gel behavior. J Am Ceram Soc 103:4140–4149
39. Coblas DG, Fatu A, Maoui A, Hajam M (2015) Manufacturing textured surfaces: State of art and recent developments. J Eng Tribology 229:3–29